*Mineralogical Magazine* (2022), **86**, 577–585
doi:10.1180/mgm.2021.96

CAMBRIDGE UNIVERSITY PRESS

## Article

## Special Issue dedicated to Peter Williams

# Sluzhenikinite, $Pd_{15}(Sb_{7-x}Sn_x)$ $3 \leq x \leq 4$, a new platinum group mineral (PGM) from the Oktyabrsk deposit, the Noril`sk deposits, Russia

Anna Vymazalová[1]*, Mark D. Welch[2], František Laufek[1], Vladimir V. Kozlov[3], Chris J. Stanley[2] and Jakub Plášil[4]

[1]Czech Geological Survey, Geologická 6, 152 00 Prague 5, Czech Republic; [2]Department of Earth Sciences, Natural History Museum, London, SW7 5BD, UK; [3]Oxford Instruments (Moscow Office), 26, Denisovskii Pereulok, Moscow, 105005, Russia; and [4]Institute of Physics ASCR, v.v.i., Na Slovance 2, 128 21 Prague 8, Czech Republic

**Abstract**

Sluzhenikinite, $Pd_{15}(Sb_{7-x}Sn_x)$ with $3 \leq x \leq 4$, is a new mineral discovered in the pegmatoidal galena–chalcopyrite massive ore from the Oktyabrsk mine, Oktyabrsk deposit of the Noril`sk deposits, Russia. Sluzhenikinite forms euhedral elongate lamellar crystals (100–150 μm long and 10–50 μm wide) associated with Au–Ag alloy, insizwaite and myrmekitic intergrowths of Pt–Pd minerals (stibiopalladinite, maslovite and sobolevskite), in close association of sperrylite and base-metal sulfides (galena, chalcopyrite, cubanite and pentlandite). In plane-polarised light, sluzhenikinite is pale brown with weak bireflectance, imperceptible pleochroism, and weak anisotropy with straw yellow to deep blue rotation tints; it exhibits no internal reflections. Reflectance values for sluzhenikinite in air ($R_1$, $R_2$ in %) are: 46.2, 46.5 at 470nm; 52.1, 52.2 at 546nm; 54.7, 55.1 at 589nm; and 57.8, 59.0 at 650nm. Thirteen electron-microprobe analyses of sluzhenikinite gave an average composition: Pd 65.06, Sn 15.60 and Sb 19.58, total 100.24 wt.%, corresponding to the formula $Pd_{14.88}(Sb_{3.92}Sn_{3.20})_{\Sigma 7.12}$ based on 22 atoms; the average of twenty-one energy dispersive spectroscopy analyses on co-type material gave: Pd 63.36, Pt 1.15, Sn 16.28 and Sb 19.21, total 100.00 wt.%, corresponding to the formula $(Pd_{14.62}Pt_{0.14})_{\Sigma 14.76}(Sb_{3.87}Sn_{3.37})_{\Sigma 7.24}$. The density, calculated on the basis of the empirical formula, is 11.22 g/cm$^3$. The mineral is monoclinic, space group $P2_1/m$, with $a = 7.5558(1)$, $b = 29.2967(3)$, $c = 7.5713(1)$ Å, $\beta = 119.931(2)°$, $V = 1452.44(4)$ Å$^3$ and $Z = 4$. The crystal structure was determined using data from single-crystal X-ray diffraction and demonstrates conclusively that the correct stoichiometry is $Pd_{15}(Sb,Sn)_7$, rather than $Pd_2(Sb,Sn)$; $R_1 = 0.035$, $wR_2 = 0.073$, GoF = 1.118 for 209 refined parameters and 4738 unique reflections. The mineral is named after Sergey Fedorovich Sluzhenikin, an expert on platinum-group minerals, particularly from the area of the type locality.

**Keywords:** sluzhenikinite, platinum-group mineral, $Pd_{15}(Sb_{7-x}Sn_x)$, Oktyabrsk mine, Oktyabrsk deposit, Noril`sk deposits, Russia

(Received 29 August 2021; accepted 2 December 2021; Accepted Manuscript published online: 22 December 2021; Associate Editor: David Hibbs)

## Introduction

Sluzhenikinite, $Pd_{15}(Sb_{7-x}Sn_x)$ with $3 \leq x \leq 4$, is a new platinum-group mineral (PGM) discovered in the pegmatitic galena–chalcopyrite massive ore from the Oktyabrsk mine (schaft No 1), Oktyabrsk deposit of the Noril`sk deposits, Russia (coordinates: 69°32′10″N, 88°27′17″E). Pegmatoidal schlieren (with up 30 vol.% of galena) occur in the upper-contact of Cu-rich orebodies of the Oktyabrsk mine and in the southern orebody in the eastern part of the Komsomolsky mine (Sluzhenikin and Mohkov, 2015). Galena forms symplectitic intergrowths with chalcopyrite; pentlandite, cubanite and fine-grained pyrrhotite are less abundant. The schlieren vary from centimetres to a few decimetres in size and have sharp boundaries with the host ore. Their shape is variable from irregular to spherical. This type of ore is rich in rare minerals such as argentopentlandite, parkerite, Pb–Tl-rich djerfisherite, thalfenisite, thalcusite, stannite, cassiterite, tellurobismuthite and breithauptite. Sluzhenikinite forms intergrowths with Sb-sobolevskite, Bi–Te geversite, Te-insizwaite, maslovite, stannopalladinite, paolovite, Sb-paolovite, altaite, hessite, native Ag and Ag–Au alloy. The size of aggregates of platinum-group minerals reach up to 4 cm in size. These types of ores are formed from residual sulfide solutions, rich in copper and volatile components (Sluzhenikin and Mohkov, 2015).

A preliminary description of a mineral having a similar composition to sluzhenikinite as an unnamed phase $Pd_4SnSb$ was given by Sluzhenikin (2011), Sluzhenikin and Mokhov (2015) and Spiridonov *et al.* (2015). The unnamed mineral UM1992–32-Sb:PdSn (Grokhovskaya *et al.*, 1992) listed in Smith and Nickel (2007) is most likely to be Sb-rich paolovite.

The new mineral and its name (symbol Szhi) were approved by the Commission on New Minerals, Nomenclature and Classification of the International Mineralogical Association (CNMNC IMA) as proposal 2020-089 (Vymazalová *et al.*, 2021).

*Author for correspondence: Anna Vymazalová, Email: anna.vymazalova@geology.cz
This paper is part of a thematic set that honours the contributions of Peter Williams
**Cite this article:** Vymazalová A., Welch M.D., Laufek F., Kozlov V.V., Stanley C.J. and Plášil J. (2022) Sluzhenikinite, $Pd_{15}(Sb_{7-x}Sn_x)$ $3 \leq x \leq 4$, a new platinum group mineral (PGM) from the Oktyabrsk deposit, the Noril`sk deposits, Russia. *Mineralogical Magazine* **86**, 577–585. https://doi.org/10.1180/mgm.2021.96

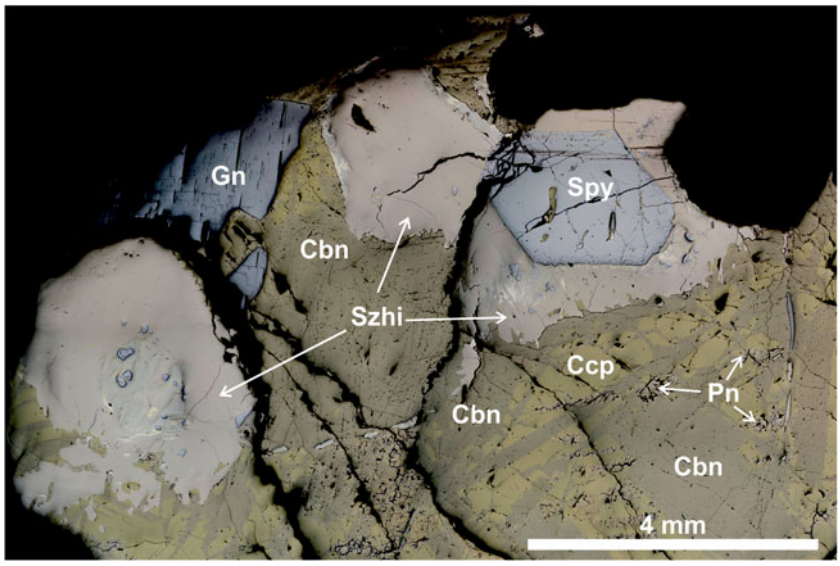


**Fig. 1.** Reflected-light microphotograph of the sample studied containing sluzhenikinite**.** Abbreviations: Szhi – sluzhenikinite, Spy – sperrylite, Cbn – cubanite, Gn – galenite and Ccp – chalcopyrite.

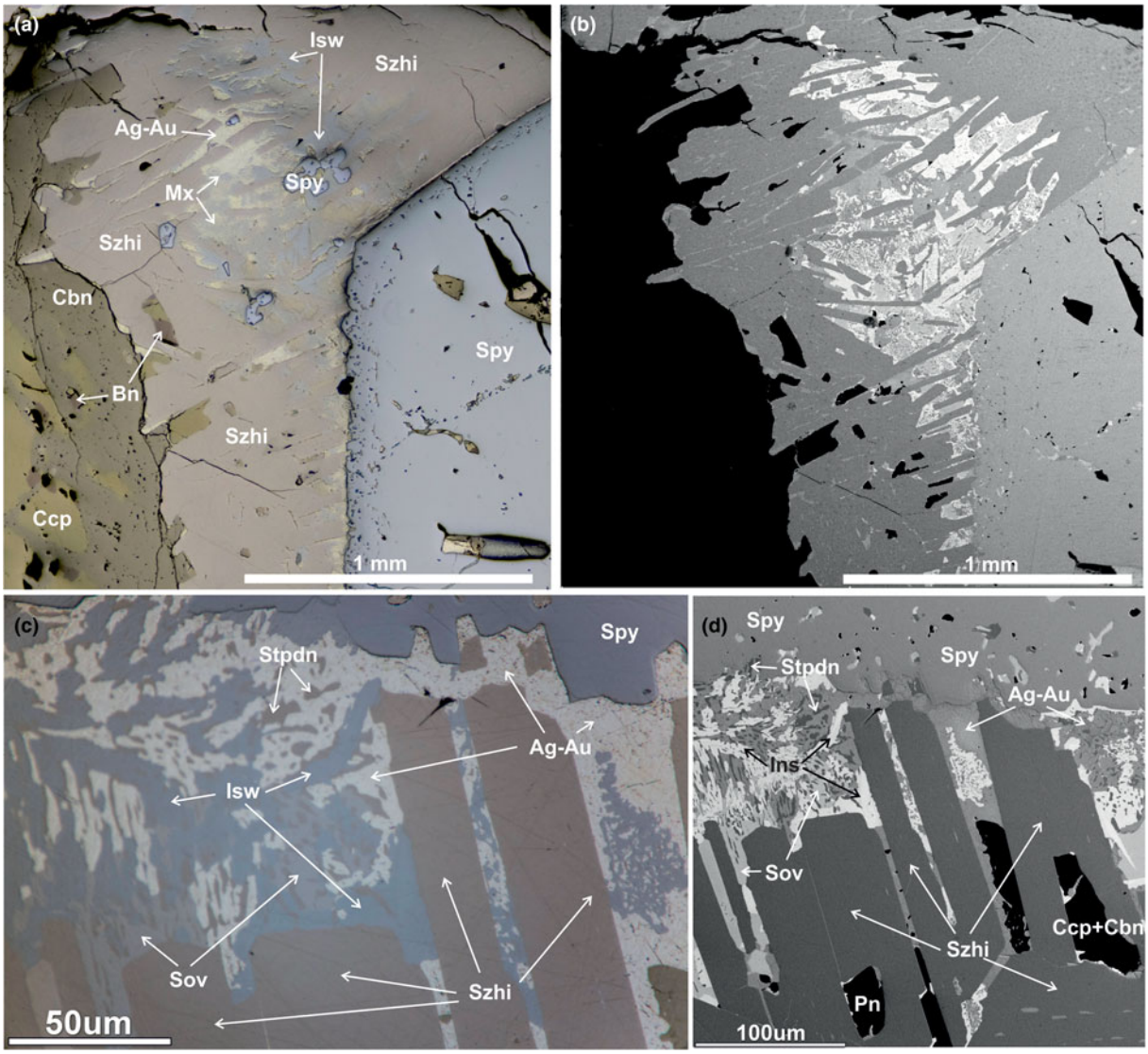


**Fig. 2.** (a, c) Reflected-light and (b, d) back-scattered electron images showing sluzhenikinite and associated minerals. (c, d) Crystals of sluzhenikinite used for collecting of X-ray data. Abbreviations: Szhi – sluzhenikinite, Isw – insizwaite, Spy – sperrylite, Sov – sobolevskite, Mx – myrmekite mixture of insizwaite, stibiopalladinite and maslovite, Stpdn – stibiopalladinite, Cbn – cubanite, Ccp –chalcopyrite and Bn – bornite.

https://doi.org/10.1180/mgm.2021.96 Published online by Cambridge University Press

**Table 1.** Reflectance data for sluzhenikinite.

| λ (nm) | $R_1$ (%) | $R_2$ (%) | λ (nm) | $R_1$ (%) | $R_2$ (%) |
|---|---|---|---|---|---|
| 400 | 40.7 | 41.3 | 560 | 52.8 | 52.9 |
| 420 | 42.2 | 42.8 | 580 | 54.0 | 54.3 |
| 440 | 43.8 | 44.3 | **589** | **54.7** | **55.1** |
| 460 | 45.4 | 45.8 | 600 | 55.3 | 55.7 |
| **470** | **46.2** | **46.5** | 620 | 56.4 | 57.0 |
| 480 | 47.0 | 47.2 | 640 | 57.3 | 58.3 |
| 500 | 48.4 | 48.6 | **650** | **57.8** | **59.0** |
| 520 | 50.0 | 50.0 | 660 | 58.2 | 59.5 |
| 540 | 51.4 | 51.5 | 680 | 59.1 | 60.7 |
| **546** | **52.1** | **52.2** | 700 | 60.0 | 62.0 |

Note: The values required by the Commission on Ore Mineralogy are given in bold.

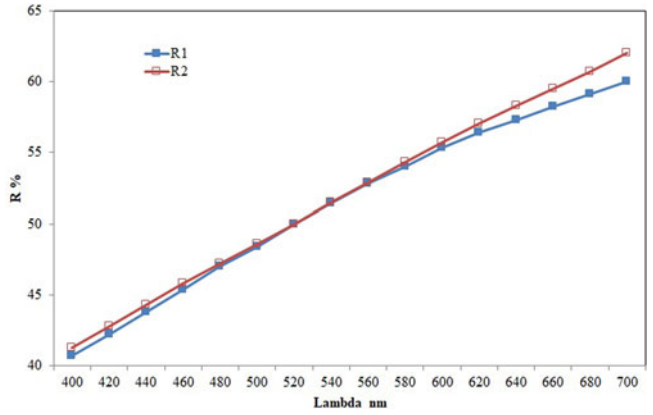


**Fig. 3.** Reflectance data of sluzhenikinite.

The mineral is named after Sergey Fedorovich Sluzhenikin (b. 1943) (Сергей Фёдорович Служеникин), research geologist at the Institute of Geology of Ore Deposits, Petrography, Mineralogy and Geochemistry of the Russian Academy of Sciences, Moscow, Russia, for his contributions to the ore mineralogy and mineral deposits of platinum-group elements, particularly from the area of the type locality, the Noril`sk deposits.

Holotype material (polished section and the single crystal used in the structure determination) is deposited in the mineralogical collection of the Natural History Museum, London, United Kingdom, catalogue number BM 2020,20 and co-type material (polished section) is deposited in the Fersman Mineralogical Museum, Moscow, Russia, under catalogue number 5691/1.

## Appearance, physical and optical properties

In polished sections, sluzhenikinite forms euhedral elongate lamellar crystals (100–150 μm long and 10–50 μm wide) associated with with Au–Ag alloy, insizwaite and myrmekitic intergrowths of Pt–Pd minerals (stibiopalladinite, maslovite and sobolevskite), in close association of sperrylite and base-metal sulfides (galena, chalcopyrite, cubanite and pentlandite). Reflected-light and back-scattered-electron images of sluzhenikinite and its associations are shown in Fig. 1 and 2, respectively. Other associated minerals are geversite, paolovite, Sb-paolovite, altaite, hessite, argentopentlandite, bornite, and pyrrhotite.

The density calculated on the basis of the empirical formula and cell dimensions of sluzhenikinite is 11.22 g.cm$^{-3}$.

**Table 2.** Chemical data (in wt. %) for sluzhenikinite.

| Constituent | Pd | Pt | Sn | Sb | Total |
|---|---|---|---|---|---|
| Type material ($n$ = 13) | | | | | |
| Average | 65.06 | | 15.6 | 19.58 | 100.24 |
| Range | 64.50–65.70 | | 14.97–16.42 | 18.72–19.96 | |
| S.D. | 0.44 | | 0.38 | 0.4 | |
| Co-type material ($n$ = 21)* | | | | | |
| Average | 63.36 | 1.15 | 16.28 | 19.21 | 100 |
| Range | 61.22–64.26 | 0–3.5 | 15.77–18.83 | 16.45–20.07 | |
| S.D. | 0.81 | 0.96 | 0.63 | 0.77 | |

S.D. – standard deviation, *EDS analyses.

In plane-polarised light, sluzhenikinite is pale brown with weak bireflectance, imperceptible pleochroism, and weak anisotropy with straw yellow to deep blue rotation tints; it exhibits no internal reflections. The reflectance measurements were made in air relative to a WTiC standard on sluzhenikinite using a J & M TIDAS diode array spectrometer attached to a Zeiss Axiotron microscope. The results are presented in Table 1 and illustrated in Fig. 3.

## Chemical composition

Electron microprobe analyses (EMPA) were performed with a CAMECA SX-100 electron probe microanalyser in wavelength-dispersive mode using an electron beam focused to 1–2 μm. Pure elements were used as standards. Concentrations were quantified on Pd*Lα*, Sb*Lα* and Sn*Mα* with an accelerating voltage of 15 kV and a beam current of 10 nA on the Faraday cup. Other elements were below the detection limit. The EMPA data were collected on four different grains of the type material ($n$ = 13). Additional energy dispersive spectroscopy (EDS) analyses ($n$ = 22) were collected on co-type material, using an EDS Aztec Energy X-Max 150 (Oxford Instruments) installed on a SEM Lyra 3GM (Tescan). The following conditions of measurements were used: voltage of 20 kV, a beam current of 0.5 nA with 500,000 counts collected for every spectrum, XPP matrix correction and pure Pd, Sn, Sb and Pt as standards. Chemical analyses for sluzhenikinite are summarised in Table 2.

The range of compositional variation of sluzhenikinite is shown in Fig. 4. It forms a narrow solid solution along the $Pd_2Sb$–$Pd_2Sn$ join indicating substitution of Sb by Sn, while Pd+Pt content remains approximately constant. Hence, the empirical composition of this solid solution can be expressed as $Pd_{15}(Sb_{7-x}Sn_x)$ with $3 \leq x \leq 4$, more specifically where $3.06 \leq x \leq 3.97$. According to our preliminary experimental results in the Pd–Sn–Sb system, there is no complete solid solution between $Pd_2Sb$ and $Pd_2Sn$. On the basis of published phase diagrams for Pd–Sb and Pd–Sn binary systems (Massalski *et al.*, 1990), sluzhenikinite does not have its structural analogue within these binary systems. Our experimental results also show, that both Sn and Sb are essential for sluzhenikinite formation.

## X-ray crystallography

### *Single-crystal X-ray diffraction*

A thin, elongate, lamellar crystal (0.145 mm × 0.025 mm × 0.010 mm) was extracted from a polished mount and attached to a 0.01 mm diameter non-diffracting carbon fibre that was glued to a 0.1 mm glass support rod. Data collection used an XcaliburE four-circle diffractometer equipped with an Eos area

https://doi.org/10.1180/mgm.2021.96 Published online by Cambridge University Press

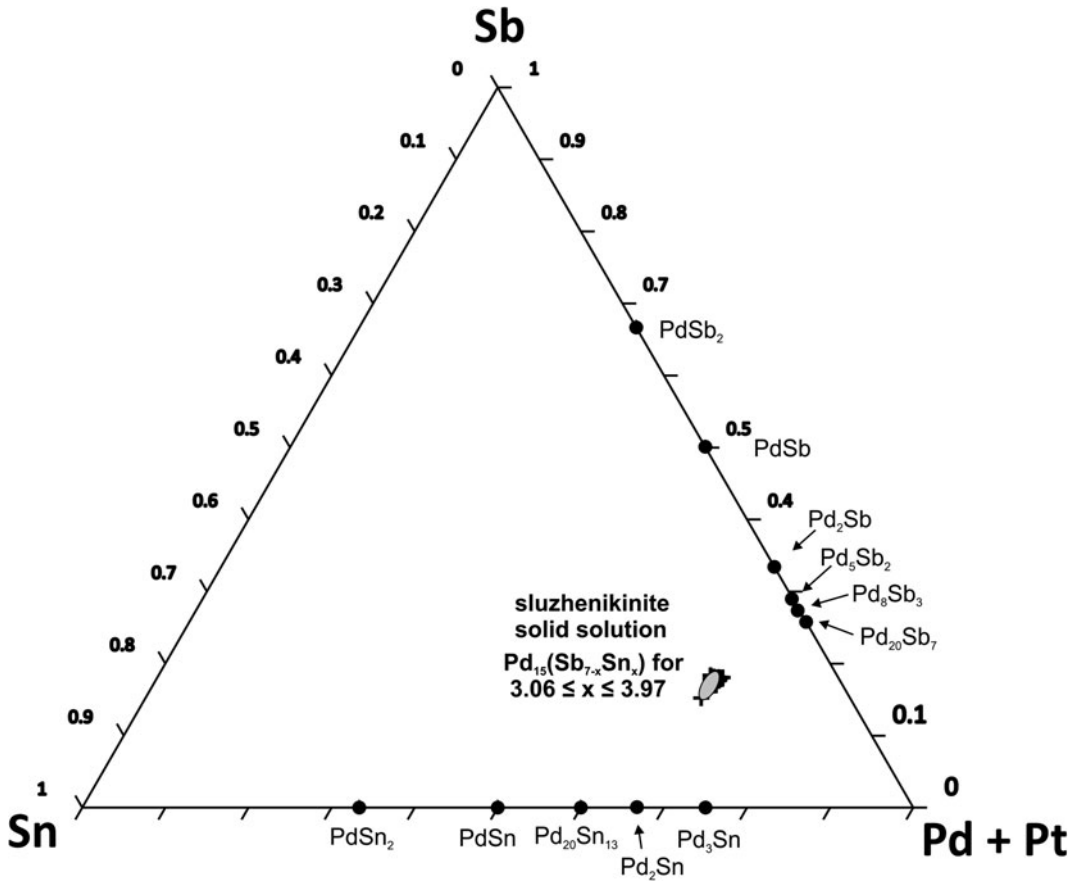


**Fig. 4.** A ternary diagram of the (Pd+Pt)–Sb–Sn system.

detector and graphite-monochromated Mo*K*α radiation operated at 50 kV and 40 mA. Raw reflection intensities were corrected for polarisation and Lorentz effects and converted to structure factors using the program *CrysalisPro*® (Rigaku Oxford Diffraction). Structure determination used *SHELX* (Sheldrick, 2008; 2015); specifically *SHELXL* version 2018/3. Neutral atomic-scattering factors taken from the *International Tables for Crystallography* (Wilson, 1992) were used.

The assignment of atom sites as Pd or Sn/Sb was based upon refined site scattering values (46 $e^-$ versus 50.5 $e^-$) and consideration of nearest interatomic distances. The ranges of plausible Pd–Pd and Pd–Sb distances were obtained from the structures of several related Pb–Sb and Pb–Sn minerals and synthetic compounds. Initially, the structure was determined in orthorhombic space group *Cmcm* and gave acceptable agreement indices, but a high GoF (1.275). A very high value of the second *SHELX* reflection-weighting parameter ($b = 256$) also indicated an inadequacy in the *Cmcm* model. Furthermore, there were 10 strong violators [$I/\sigma(I) > 7$, the strongest has $I \approx 28\sigma(I)$] of the *c*-glide. Consequently, a structure solution was sought in the most closely related sub-group of *Cmcm*, namely a monoclinic $P2_1/m$ structure with half the volume of the orthorhombic unit-cell and related to the latter by the transformation matrix [½½0/00$\bar{1}$/½$\bar{½}$0]. The $P2_1/m$ model led to an excellent refined structure and much lower value of $b = 26$. This value is, nonetheless, somewhat high and may reflect an inability to distinguish Sb and Sn over the eight non-equivalent Sb/Sn sites in the structure. We also attempted to refine the structure in a monoclinic $C2/m$ derivative of *Cmcm*, but this model failed to lead to a stable refinement or to give a plausible structure.

A close hexagonal/orthorhombic/monoclinic metric pseudo-symmetry is a common feature of this family of Pd–Sb minerals. As there is a very close corresponding hexagonal metric [$a$ = 7.5662(1) Å and $c$ = 29.2932(6) Å], we also carried out data reduction in hexagonal space groups. However, merging of symmetry-equivalent reflections was very poor. For example, we used the space group of stibiopalladinite $Pd_5Sb_2$, $P6_3cm$ (non-centrosymmetric), which has a cell metric ($a$ = 7.598 Å and $c$ = 28.112 Å) near that of sluzhenikinite and we obtained a very high $R_{int}$ value of 0.44 for merging in point group 6*mm*. Trigonal and other hexagonal point groups also gave very poor reflection merging, e.g. 6/*m*, $\bar{3}$ and $\bar{3}m$, had $R_{int} = 0.42$. *E*-statistics, which should work well for sluzhenikinite as Pd, Sn and Sb have very similar atomic numbers, indicated that the structure is highly likely (79% probability) to be centrosymmetric. Clearly, the stibiopalladinite space group is not relevant for sluzhenikinite. The poor reflection merging for hexagonal/trigonal point groups also excludes hexagonal/trigonal symmetry. Consequently, after a thorough exploration of possible options, we consider the monoclinic ($P2_1/m$) model to be most appropriate for sluzhenikinite.

All atoms of the monoclinic structure were found by structure solution using direct methods and were initially assigned to Pd. Examination of isotropic displacement factors indicated that some sites had much lower values than others, suggesting occupancy by a more electron-rich element, namely Sn/Sb. Residual electron-density maxima of 3–4 $e^-/Å^3$ in difference-Fourier maps

https://doi.org/10.1180/mgm.2021.96 Published online by Cambridge University Press

**Table 3.** Information relating to the data collection and structure refinement of sluzhenikinite.

| | |
|---|---|
| **Crystal data** | |
| Ideal formula | $Pd_{15}(Sn,Sb)_7$ |
| Empirical formula (EMPA)* | $Pd_{14.88}Sn_{3.20}Sb_{3.92}$ |
| Crystal system, space group | Monoclinic, $P2_1/m$ (No. 11) |
| $a$ (Å) | 7.5558(1) |
| $b$ (Å) | 29.2967(3) |
| $c$ (Å) | 7.5713(1) |
| β (°) | 119.931(2) |
| $V$ (Å$^3$) | 1452.44(4) |
| $Z$ | 4 |
| **Data collection** | |
| Diffractometer | Xcalibur E (1K Eos detector) |
| Radiation | MoKα |
| Crystal | Thin rectangular metallic blade |
| Max. Med. Min. dimensions (mm) | 0.145, 0.025, 0.010 |
| Temperature (K) | 293(2) |
| Scan type, frame-width (°), frame-time (s) | ω, 0.75, 130 |
| Absorption correction | Multi-scan |
| $T_{min}$, $T_{max}$ | 0.2131, 1 |
| Reflections used for cell, $I$ >7σ($I$) | |
| Reflections measured | 30480 |
| $R_\sigma$ | 0.021 |
| Independent reflections | 4738 |
| Independent reflections with $I$ >2σ($I$) | 4216 |
| $R_{int}$ | 0.038 |
| θ $_{min}$, θ $_{max}$ (°) | 3.11, 31.77 |
| Index range | $h$ ±11, $k$ ±41, $l$ −10, +11 |
| Data completeness to 30°θ (%) | 99.6 |
| **Refinement** | |
| Reflections, restraints, parameters | 4738, 0, 209 |
| $R_1[I > 2\sigma(I)]$, $R_1$(all) | 0.030, 0.035 |
| $wR_2[I > 2\sigma(I)]$, $wR_2$(all) | 0.070, 0.073 |
| $S(F^2)$ | 1.118 |
| Reflection weighting coefficients $a$, $b$** | 0.0270, 26.77 |
| $(\Delta/\sigma)_{max}$ | < 0.001 |
| $\Delta\rho_{max}$, $\Delta\rho_{min}$ ($e$ Å$^{-3}$) | +3.4, −2.0 |

*Average of 13 analyses by electron microprobe (WDS) calculated to 22 atoms per formula.
**SHELX

**Table 4.** Atom coordinates and equivalent-isotropic displacement parameters (Å$^2$) for sluzhenikinite (in reality Sb positions represent Sb/Sn mixed positions).

| Site | $x$ | $y$ | $z$ | $U_{eq}$ |
|---|---|---|---|---|
| Pd1 | 0.1532(1) | ¼ | 0.5000(1) | 0.0104(1) |
| Pd2 | −0.13770(8) | 0.09568(2) | 0.12280(8) | 0.0107(1) |
| Pd3 | 0.87152(8) | 0.09264(2) | 0.49996(9) | 0.0112(1) |
| Pd4 | 0.17745(8) | 0.03594(2) | 0.14354(8) | 0.0124(1) |
| Pd5 | 0.53397(8) | 0.03593(2) | 0.85654(9) | 0.0123(1) |
| Pd6 | −0.12375(8) | 0.00001(2) | 0.25262(8) | 0.0120(1) |
| Pd7 | 0.56224(8) | 0.14869(2) | 0.19854(8) | 0.0099(1) |
| Pd8 | −0.13624(8) | 0.14870(2) | −0.19857(8) | 0.0098(1) |
| Pd9 | 0.23469(9) | 0.19827(2) | −0.12950(9) | 0.0107(1) |
| Pd10 | 0.49420(9) | 0.19864(2) | 0.50006(9) | 0.0110(1) |
| Pd11 | −0.13577(9) | 0.19828(2) | 0.12954(9) | 0.0106(1) |
| Pd12 | −0.1354(1) | ¼ | −0.2106(1) | 0.0107(1) |
| Pd13 | 0.5753(1) | ¼ | 0.2107(1) | 0.0107(1) |
| Pd14 | ½ | 0 | ½ | 0.0193(2) |
| Pd15 | 0.49607(9) | 0.09751(2) | 0.50009(9) | 0.0111(1) |
| Pd16 | 0.23952(8) | 0.09567(2) | −0.12282(8) | 0.0105(1) |
| Pd17 | 0.16975(7) | 0.14864(2) | 0.50002(8) | 0.0058(1) |
| Sb1 | 0.19522(7) | 0.14365(2) | 0.16481(8) | 0.0117(1) |
| Sb2 | 0.53043(7) | 0.14367(2) | 0.83526(7) | 0.0116(1) |
| Sb3 | −0.13410(7) | 0.19186(2) | 0.50003(7) | 0.0093(1) |
| Sb4 | 0.18626(7) | 0.05421(2) | 0.50003(8) | 0.0108(1) |
| Sb5 | 0.55072(7) | 0.05367(2) | 0.20371(7) | 0.0104(1) |
| Sb6 | −0.15301(7) | 0.05365(2) | −0.20375(7) | 0.0104(1) |
| Sb7 | 0.1977(1) | ¼ | 0.1664(1) | 0.0090(1) |
| Sb8 | 0.5313(1) | ¼ | 0.8336(1) | 0.0092(1) |

**Table 5.** Calculated powder X-ray diffraction values for sluzhenikinite ($d$, Å, $I$, %)*.

| $I_{calc}$ | $d_{calc}$ | $h$ $k$ $l$ | $I_{calc}$ | $d_{calc}$ | $h$ $k$ $l$ |
|---|---|---|---|---|---|
| 2 | 3.1977 | 0 8 1 | 6 | 1.9712 | $\bar{2}$ 9 3 |
| 3 | 2.9941 | 0 4 2 | 2 | 1.9694 | $\bar{3}$ 9 1 |
| 5 | 2.9296 | 0 10 0 | 4 | 1.9694 | $\bar{3}$ 9 2 |
| 6 | 2.9148 | 1 9 0 | 4 | 1.9365 | 1 13 1 |
| 6 | 2.9148 | $\bar{1}$ 9 1 | 4 | 1.9364 | $\bar{1}$ 13 2 |
| 8 | 2.6751 | 0 10 1 | 4 | 1.9364 | $\bar{3}$ 10 1 |
| 3 | 2.6742 | 1 10 0 | 4 | 1.8899 | $\bar{3}$ 10 2 |
| 3 | 2.6742 | $\bar{1}$ 10 1 | 2 | 1.8117 | $\bar{4}$ 1 1 |
| 5 | 2.4771 | 2 0 1 | 2 | 1.8117 | $\bar{4}$ 1 3 |
| 5 | 2.477 | $\bar{2}$ 0 3 | 3 | 1.7526 | 0 10 3 |
| 5 | 2.4705 | 1 1 2 | 2 | 1.7503 | 3 10 0 |
| 5 | 2.4704 | $\bar{1}$ 1 3 | 2 | 1.7503 | $\bar{3}$ 10 3 |
| 5 | 2.4682 | 1 9 1 | 5 | 1.6338 | $\bar{4}$ 9 2 |
| 4 | 2.4682 | $\bar{1}$ 9 2 | 4 | 1.6276 | 0 18 0 |
| 4 | 2.466 | $\bar{2}$ 9 1 | **16** | **1.5899** | **2 10 2** |
| 4 | 2.4647 | $\bar{3}$ 1 1 | **16** | **1.5899** | **$\bar{2}$ 10 4** |
| 4 | 2.4646 | $\bar{3}$ 1 2 | 4 | 1.5876 | $\bar{4}$ 10 2 |
| 3 | 2.4445 | 1 2 2 | 7 | 1.54077 | $\bar{4}$ 11 2 |
| 3 | 2.4445 | $\bar{1}$ 2 3 | **19** | **1.4648** | **0 20 0** |
| 7 | 2.4436 | 0 8 2 | 7 | 1.3658 | 2 9 3 |
| 3 | 2.3484 | 1 4 2 | 7 | 1.3658 | $\bar{2}$ 9 5 |
| 3 | 2.3484 | $\bar{1}$ 4 3 | 2 | 1.3652 | 3 9 2 |
| **65** | **2.3169** | **1 10 1** | 2 | 1.3652 | $\bar{3}$ 9 5 |
| **65** | **2.3169** | **$\bar{1}$ 10 2** | 5 | 1.3632 | $\bar{5}$ 9 2 |
| **100** | **2.3151** | **$\bar{2}$ 10 1** | 5 | 1.3632 | $\bar{5}$ 9 3 |
| **29** | **2.3084** | **2 9 0** | 3 | 1.3379 | 3 10 2 |
| **29** | **2.3084** | **$\bar{2}$ 9 2** | 3 | 1.3379 | $\bar{3}$ 10 5 |
| 3 | 2.2106 | 1 6 2 | 2 | 1.309 | 1 21 1 |
| 3 | 2.2106 | $\bar{1}$ 6 3 | 2 | 1.309 | $\bar{2}$ 21 2 |
| **89** | **2.1872** | **0 0 3** | 3 | 1.308 | $\bar{5}$ 9 1 |
| 22 | 2.1852 | 0 10 2 | 3 | 1.3079 | $\bar{5}$ 9 4 |
| **74** | **2.1827** | **3 0 0** | 4 | 1.3057 | 0 18 3 |
| **74** | **2.1826** | **$\bar{3}$ 0 3** | 3 | 1.2863 | 1 10 4 |
| **15** | **2.1783** | **1 11 1** | 3 | 1.2863 | $\bar{1}$ 10 5 |
| **25** | **2.1766** | **$\bar{1}$ 11 2** | 5 | 1.2839 | $\bar{5}$ 10 1 |
| 3 | 2.1301 | 3 3 0 | 5 | 1.2839 | $\bar{5}$ 10 4 |
| 3 | 2.13 | $\bar{3}$ 3 3 | 5 | 1.2619 | 3 0 3 |
| 4 | 2.0661 | 2 11 0 | 5 | 1.2619 | $\bar{3}$ 0 6 |
| 4 | 2.0661 | $\bar{2}$ 11 2 | 2 | 1.2596 | 4 11 1 |
| 4 | 2.053 | 1 8 2 | 2 | 1.2594 | $\bar{4}$ 11 5 |
| 4 | 2.053 | $\bar{1}$ 8 3 | 4 | 1.2594 | 3 19 0 |

*Calculated using *PowderCell 2.3* (Krause and Nolze, 1996; Nolze, 2017). The strongest bands are given in bold.

were located within 0.4 Å of Pd atoms, confirming the presence of an element of higher atomic number. However, due to the almost identical atomic numbers of Sn (50) and Sb (51), it was not possible to distinguish between these two elements. Consequently, the non-Pd sites were modelled as Sb. Pd17 was modelled as either Pd or Sb. When Pd17 = Sb there is a corresponding electron density minimum of −2 $e^-$/Å$^3$. When Pd17 = Pd there is a corresponding maximum of 3 $e^-$/Å$^3$ at 0.36 Å away from Pd17. The site-scattering value obtained by refining Sb or Pd occupancy is 48 electrons (0.97Sb or 1.04Pd). However, consideration of interatomic distances implies that the occupant of Pd17 is Pd or Pd-dominant. It is conceivable that the minor amount of Pt ($Z$ = 78) found by EMPA is ordered at this site, which would lead to a small increase in site-scattering value. In addition to the +3 $e^-$/Å$^3$ maximum at Pd17, the twenty highest residual electron-density maxima in the difference-Fourier map for the final refinement have values between +1.4 and +2.1 $e^-$/Å$^3$; the most negative electron density difference is −1.9 $e^-$/Å$^3$.

Lastly, given the close metric pseudosymmetry of orthorhombic and monoclinic cells, we anticipated that the crystal could be twinned. Searches for monoclinic/orthorhombic-$C$ and monoclinic/hexagonal

https://doi.org/10.1180/mgm.2021.96 Published online by Cambridge University Press

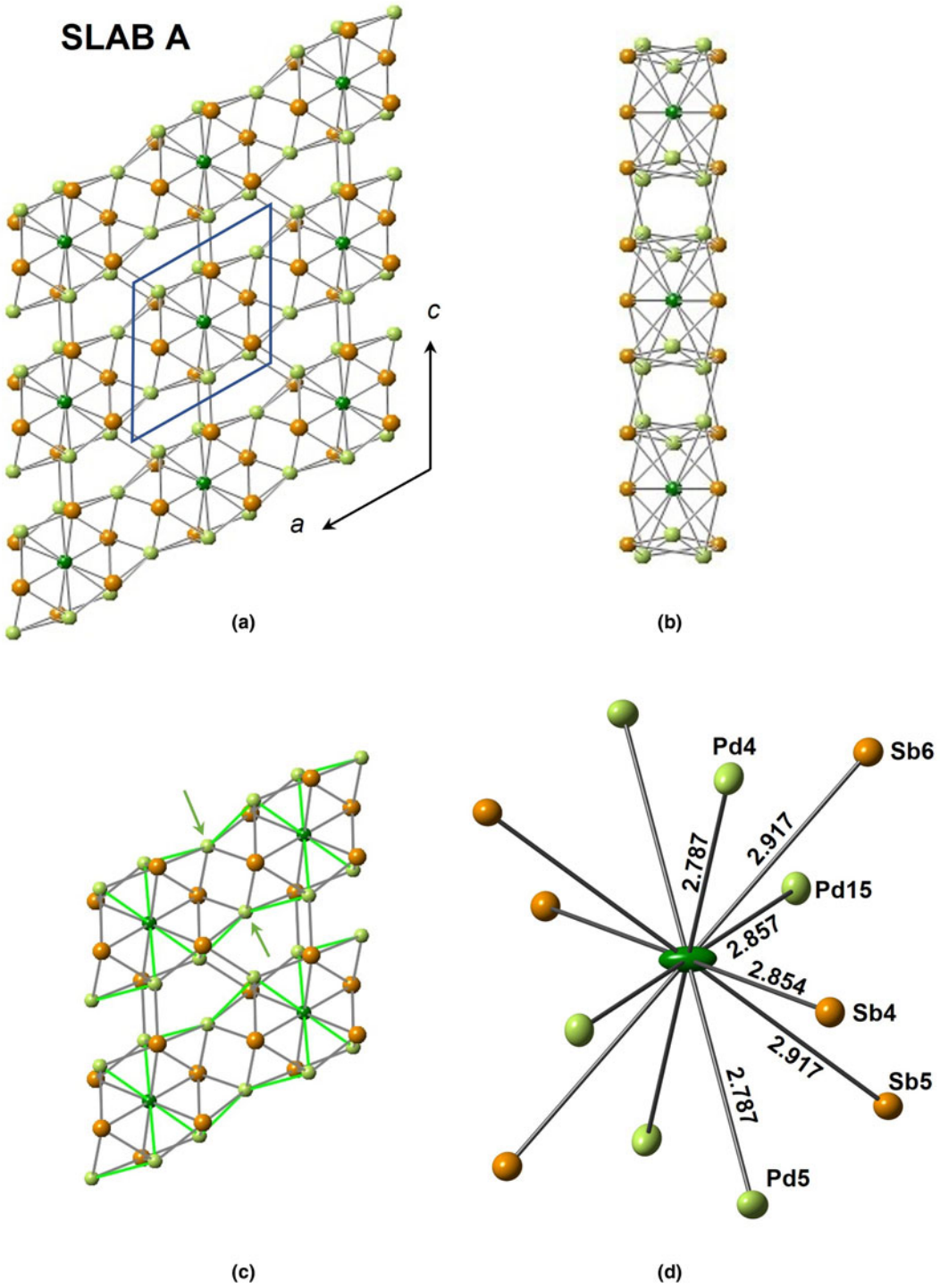


**Fig. 5.** The three different structural modules of sluzhenikinite. (a) Slab A projected onto (010). Rows of Pd14[$Pd_4Sb_6$] polyhedra extend parallel to [100]. (b) A view of the slab looking along the *a*-axis and showing tunnels extending parallel to [100]. (c) Close-up of the linkages between polyhedra involving pairs of Pd atoms (arrowed) within a row and Pd–(Sn,Sb) bonds between rows. (d) A Pd14[$Pd_6Sb_6$] polyhedron. Atom displacement ellipsoids are shown at the 68% level.

twinning for known twin laws using *CrysalisPro*® (based upon reflection intensities) did not reveal the presence of twins. Furthermore, none of the small residual unmodelled electron-density maxima could be mapped onto a possible twin. The close agreement between values of observed and calculated structure factors for the final refinement does not suggest twinning ($F_{obs}$ >> $F_{calc}$ if missed twinning is present, which is not the case here).

From a crystallographic viewpoint there are two plausible stoichiometries, depending upon how Pd17 is assigned: if Pd17 is Sb then the implied formula is $Pd_7(Sn,Sb)_4$; if Pd17 is Pd then the implied formula is $Pd_{15}(Sn,Sb)_7$. The well-defined composition determined by EMPA, $Pd_{14.88}(Sn_{3.20}Sb_{3.92})_{\Sigma 7.12}$, leads to the clear choice of $Pd_{15}(Sn,Sb)_7$ as the correct ideal formula, implying that that Pd17 is Pd. Further topological support for the

https://doi.org/10.1180/mgm.2021.96 Published online by Cambridge University Press

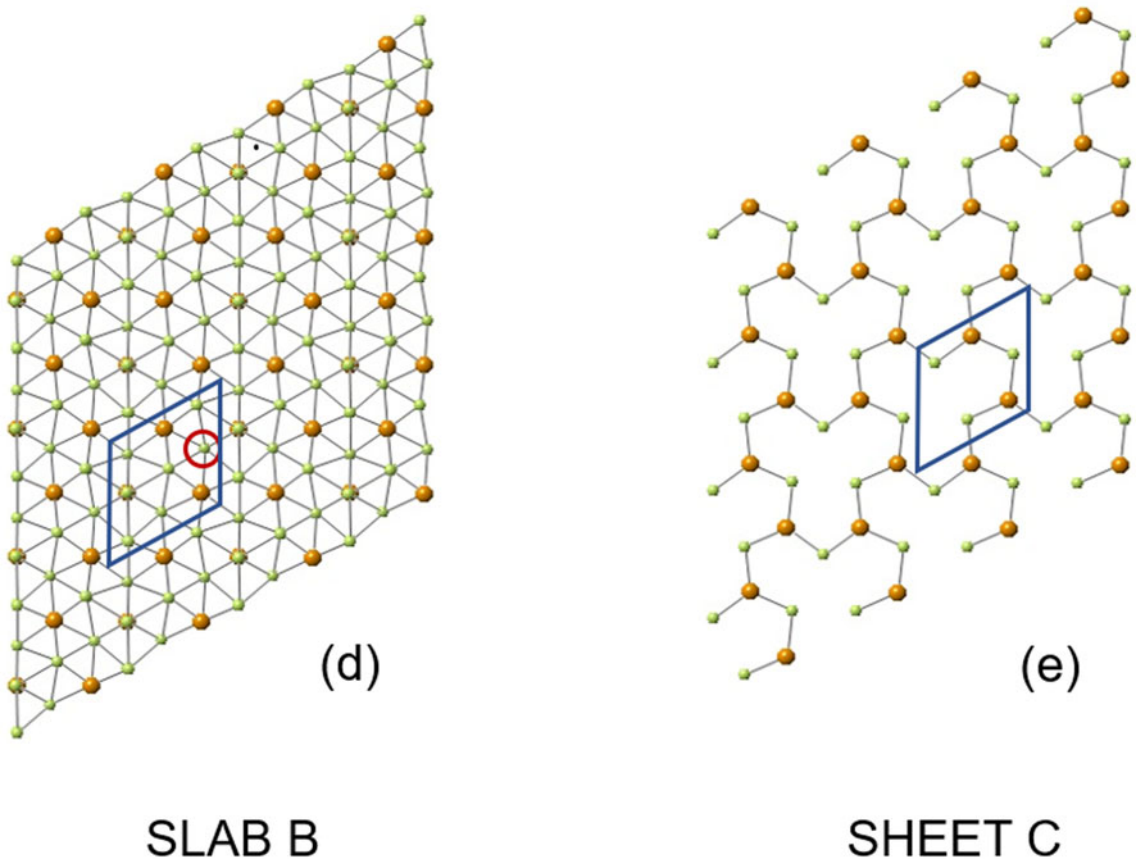


**Fig. 6.** (a) Slab B composed of a puckered sheet of (Sn,Sb) atoms defining a centred-pseudohexagonal motif and bonded to Pd atoms, (Sn,Sb) atoms are bonded to nine Pd atoms; Pd atoms are bonded to six other Pd atoms and three (Sn,Sb) atoms. (b) Sheet C comprising chains of alternating Pd and (Sn,Sb) atoms extending parallel to [001] and linked by rows of Pd atoms. See text for further details.

identification of Pd17 as Pd is discussed below. Information summarising the details of the crystal, data collection and structure refinement are given in Table 3. Atom coordinates and equivalent-isotropic displacement parameters are given in Table 4. $U_{ij}$ and interatomic distances can be found in the accompanying crystallography information file (deposited with the Principal Editors of *Mineralogical Magazine* and available as Supplementary material – see below). Calculated *d* spacings and intensities for powder X-ray diffraction, calculated using *PowderCell 2.3* (Krause and Nolze, 1996; Nolze, 2017), are shown in Table 5.

## Structure description

There are seventeen non-equivalent Pd sites and eight non-equivalent (Sb,Sn) sites in the crystal structure. Nineteen of these sites are on general positions and have a multiplicity of four; six sites (Pd1, Pd12, Pd13, Pd14, Sb7 and Sb8) lie within mirror planes and have a multiplicity of two.

The structure of sluzhenikinite is shown in Figs 5, 6 and 7. It is composed of three distinct lamellar components: slab A = $Pd_7(Sn,Sb)_6$; slab B = $Pd_{10}(Sn,Sb)_3$; and sheet C = $Pd_3(Sn,Sb)_2$.

These three components are stacked regularly along the **y** axis ….ABCBA…. in the ratio $AB_2C$, giving a corresponding overall composition $Pd_7(Sn,Sb)_6 + 2[Pd_{10}(Sn,Sb)_3] + Pd_3(Sn,Sb)_2 = Pd_{30}(Sn,Sb)_{14}$. The three components are structurally very different as we now describe.

Slab A (Fig. 5) comprises rows of $Pd_6[Sn,Sb]_6$ polyhedra with a central Pd14 atom shown in dark green in this figure. These polyhedra are connected *via* pairs of additional Pd atoms to form a row, leading to a composition $Pd_7(Sn,Sb)_6$ for the row (and slab). Adjacent rows are linked *via* Pd–(Sn,Sb) bonds. This slab has tunnels running parallel to [100] (Fig. 5b).

Slab B (Fig. 6) is composed of Pd atoms coordinated by six Pd and three (Sn,Sb) atoms; (Sn,Sb) atoms are coordinated by nine Pd atoms. The (Sn,Sb) atoms form a puckered centred-pseudohexagonal motif. In this figure the central Pd and Sb,Sn atoms are superimposed. The red circle shows the Pd17 site. The assignment of this site to Pd is discussed in the text and is consistent with the simple motif of this slab. There are two B slabs per unit cell.

Sheet C (Fig. 6e) is a single layer of atoms thick and lies wholly within the mirror plane. All three non-equivalent Pd atoms (Pd1, Pd12, Pd13) are coordinated to six Pd and four Sb/Sn atoms. Atoms Sb/Sn 7 and 8 are coordinated to nine Pd atoms.

The modular structure of sluzhenikinite (Fig. 7) suggests the possibility of a polysomatic series of Pd–Sn–Sb phases in which different proportions of these modules occur.

It is conceivable that Sn and Sb are partitioned differently between these three structural components. If this were the case, then a range of structures (polysomes) with different Sn/Sb ratios could occur.

https://doi.org/10.1180/mgm.2021.96 Published online by Cambridge University Press

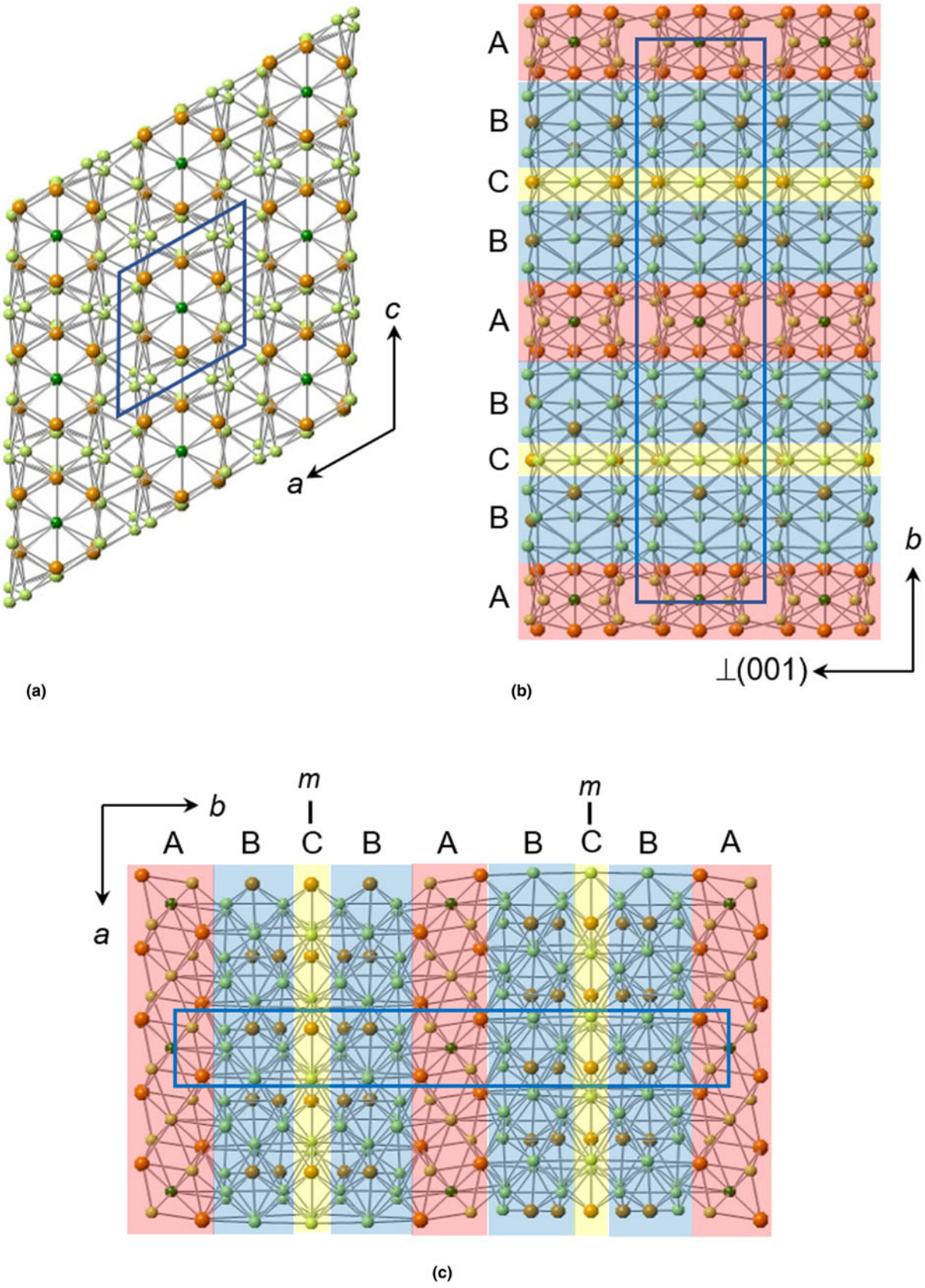


**Fig. 7.** The modular structure of sluzhenikinite showing the sequence of A, B and C modules stacked along [010] in ratio $AB_2C$. (a) Structure projected onto (010) and showing pseudohexagonal 'channels' running parallel to the *b*-axis and occupied by Pd14 and (Sn,Sb) atoms. (b) Structure viewed along the *x* axis and showing the module stacking sequence. Vacant tunnels extend parallel to [100]. (c) Structure projected onto (001) and showing the module stacking sequence.

https://doi.org/10.1180/mgm.2021.96 Published online by Cambridge University Press

**Table 6.** Unit-cell parameters (Å,°) of sluzhenikinite and related Pd–Sb–Sn minerals.

| | Formula | Space group | *a* | *b* | *c* | β |
|---|---|---|---|---|---|---|
| Naldrettite | $Pd_2Sb$ | $Cmc2_1$ | 3.391 | 17.555 | 6.957 | 90 |
| Synthetic* | $Pd_8Sb_3$ | $R\bar{3}c$ | 7.6152 | 7.6152 | 43.032 | 90 |
| Stibiopalladinite | $Pd_5Sb_2$ | $P6_3cm$ | 7.598 | 7.598 | 28.112 | 90 |
| Synthetic | $Pd_2Sn$ | *Pnma* | 5.728 | 4.33 | 8.39 | 90 |
| Synthetic** | $Pd_{20}Sb_7$ | $R\bar{3}$ | 11.734 | 11.734 | 11.021 | 90 |
| Sluzhenikinite | $Pd_{15}(Sn, Sb)_7$ | $P2_1/m$ | 7.5557 | 29.2967 | 7.5713 | 119.93 |

*Isostructural with mertieite-II, $Pd_8Sb_{2.5}As_{0.5}$.
**Isostructural with keithconnite, $Pd_{20}Te_7$.

## Relation to other minerals

There are several Pd-dominant Pd–Sn–Sb minerals and synthetic phases (Table 6): Mertieite $Pd_8Sb_3$, naldrettite $Pd_2Sb$, stibiopalladinite $Pd_5Sb_2$, synthetic $Pd_2Sn$ and synthetic $Pd_{20}Sb_7$. The latter is the Sb-analogue of keithconnite $Pd_{20}Te_7$. The Pd–Pd and Pd–Sn/Sb interatomic distances are in the ranges 2.8–3.1 Å and 2.5–3.0 Å, respectively. The corresponding distances in sluzhenikinite fall within these ranges (see supplementary crystallography information file). The narrowest range of interatomic distances is in $Pd_2Sn$ for which *d*(Pd–Pd) is 2.8–3.0 Å and *d*(Pd–Sn) is 2.7–3.0 Å. The shortest Sb(Sn)–Sb(Sn) distance in sluzhenikinite is 3.115 Å and as such is not considered to constitute a bond. Hence, there are no Sb(Sn)–Sb(Sn) bonds in sluzhenikinite, which is also true of other Pd–Sb(Sn) structures. Topologically, sluzhenikinite is unlike other Pd–Sn–Sb structures, while sharing basic features such as comparable Pd–Pd and Pd–(Sn,Sb) interatomic distances. We suggest that sluzhenikinite should belong to the 01.AG PGE-metal alloys group of the Nickel and Strunz classification.

**Acknowledgments.** We would like to take this opportunity to acknowledge the major contribution of Pete Williams to the international mineralogical community and the many fruitful shared projects, discussions and IMA-related interactions with him over the past 15 years. We acknowledge Ritsuro Miyawaki, Chairman of the CNMNC of IMA and its members for helpful comments on the original proposal. We thank Luca Bindi, Peter Leverett and an anonymous reviewer for their very helpful comments and suggestions. This research was supported by the Grant Agency of the Czech Republic (project No. 22-26485S to A.V.), by the Czech Geological Survey (DKRVO/ČGS 2018–2022). Chris Stanley acknowledges Natural Environment Research Council grant NE/M010848/1 Tellurium and selenium cycling and supply. J.P. acknowledges CzechNanoLab Research Infrastructure supported by MEYS CR (LM2018110) for financial support for the collection of diffraction data.

**Supplementary material.** To view supplementary material for this article, please visit https://doi.org/10.1180/mgm.2021.96

## References

Grokhovskaya T.L., Distler V.V., Klyunin S.F., Zakharov A.A. and Laputina I.I. (1992) Low-sulfide platinum group mineralization of the Lukkulaisvaara pluton, northern Karelia. *Geologiya Rudnykh Mestorozhdeniy*, **2**, 32–50.

Kraus W. and Nolze G. (1996) POWDER CELL – a program for the representation and manipulation of crystal structures and calculation of the resulting X-ray powder patterns. *Journal of Applied Crystallography*, **29**, 301–303.

Massalski T.N., Okamoto H., Subramanian P.R. and Kacprzak L. (editors) (1990) *Binary Alloy Phase Diagrams*, 2nd Edition. ASM International, Ohio, USA.

Nolze G. (2017) PowderCell instruction manual. *Federal Institute for Materials Research and Testing*.

Sheldrick G.M. (2008) A short history of SHELX. *Acta Crystallographica*, **A64**, 112–122.

Sheldrick G.M. (2015) Crystal structure refinement with SHELXL. *Acta Crystallographica*, **C71**, 3–8.

Sluzhenikin S.F. (2011) Platinum-copper-nickel and platinum ores of Noril`sk region and their ore mineralization. *Russian Journal of General Chemistry*, **81**, 1288–1301.

Sluzhenikin S.F. and Mokhov A.V. (2015) Gold and silver in PGE-Cu-Ni and PGE pres of the Noril`sk deposit, Russia. *Mineralium Deposita*, **50**, 465–492.

Smith D.G.W. and Nickel E.H. (2007) A system for codification for unnamed minerals: report of the Subcommittee for Unnamed Minerals of the IMA Commission on New Minerals, Nomenclature and Classification. *The Canadian Mineralogist*, **45**, 983–1055.

Spiridonov E.M., Kulagov E.A., Serova A.A., Kulikova I.M., Korotaeva N.N., Sereda E.V., Tushentsova I.N., Belyakov S.N. and Zhukov N.N. (2015) Genetic Pd, Pt, Au, Ag, and Rh mineralogy in Noril`sk sulfide ores. *Geology of Ore Deposits*, **57**, 402–432.

Vymazalová A., Welch M.D., Laufek F., Kozlov V.V., Stanley C.J. and Plášil J. (2021) Sluzhenikinite, IMA 2020-089. CNMNC Newsletter, *Mineralogical Magazine*, **85**, 454–458.

Wilson A.J.C. (editor) (1992) *International Tables for Crystallography, Volume C: Mathematical, Physical and Chemical Tables*. Kluwer Academic, Dordrecht, The Netherlands.